RSC Advances

ROYAL SOCIETY OF CHEMISTRY

www.rsc.org/advances

RSC Advances

PAPER

Received 00th January 20xx,
Accepted 00th January 20xx

DOI: 10.1039/x0xx00000x

www.rsc.org/

Microwave Assisted Synthesis of High-surface Area WO_3 Particles Decorated with Mosaic Patterns via Hydrochloric Acid Treatment of $Bi_2W_2O_9$

Fuminao Kishimoto,[a, b] Dai Mochizuki,[a, c] Masato M Maitani,[a] Eiichi Suzuki[a] and Yuji Wada[a]

Monoclinic WO_3 particles with mosaic structures on the planes of the particles were synthesized from layered bismuth tungstate ($Bi_2W_2O_9$) with the alternate stacked structure of $Bi_2O_2^{2+}$ layers and $W_2O_7^{2-}$ layers via a hydrothermal technique using hydrochloric acid at 200 °C under microwave heating. These particles possessed high surface areas, giving the high photocatalytic activity in the degradation of gaseous acetaldehyde. Sequential SEM observations have clarified the dynamic transformations of the structures of $Bi_2W_2O_9$ under microwave heating in comparison with conventional heating. The WO_3 production through the reaction of $Bi_2W_2O_9$ with HCl consists of the two reaction steps, *i.e.*, $H_2W_2O_7$ generation via replacement of $Bi_2O_2^{2+}$ with H^+ (the first step) and the conversion of $H_2W_2O_7$ to WO_3 through dehydration of $H_2W_2O_7$ (the second step). The first step proceeds even at room temperature, while the second reaction requires the temperatures above 180 °C. To investigate the microwave heating effect on the first step (the replacement of $Bi_2O_2^{2+}$), the reaction of $Bi_2W_2O_9$ and HCl was carried out at 80 °C under both microwave heating and conventional heating. It has been found that the replacement of $Bi_2O_2^{2+}$ with H^+ is accelerated by microwave selective heating effect. Interestingly, the WO_3 particles with mosaic patterns were produced only under microwave heating. On the other hand, conventional heating of $Bi_2W_2O_9$ in the presence of HCl resulted in the formation of plate-like WO_3 particles without mosaic patterns.

Introduction

Tungsten trioxides (WO_3) are n-type semiconductor with the band gap of 2.6 eV, resulting in the visible light absorption. Therefore it is widely used as a visible light responsive photo-catalyst and an anode electrode material of photovoltaic devices.[1-10] Especially, WO_3 is recognized as a characteristic catalyst enabling oxygen generation in Z-Scheme type photo-catalytic systems.[6-10] The photo-catalytic activity of WO_3 is as high as TiO_2 under UV light irradiation, and higher than N-doped TiO_2 under visible light irradiation.[11] Although this compound is considered to be conventional, it has still been attracting much interests of the researchers working on photocatalysis. Actually some researches produced the WO_3 particles with high surface areas by controlling the geometry or morphology of particles in order to improve the photo-catalytic activity of WO_3 particles.[12-15] Recently, Ueda *et al.* obtained three dimensionally ordered macroporous (3DOM) tungsten oxides with high surface area (up to 62 $m^2 g^{-1}$) by a high temperature treatment of tungsten precursor ($(NH_4)_3H_2W_{12}O_{40}$, WCl_6, $W(OEt)_5$ or $H_3PW_{12}O_{40}$) coated on poly-methyl methacrylate (PMMA).[15] The photo-catalytic performance of the 3DOM WO_3 was uplifted relative to WO_3 particles prepared without PMMA. Other metal oxides (Fe_2O_3, CeO_2, ZnO, etc.) with 3DOM structures were also prepared by the similar procedure to 3DOM.[16] Furthermore, WO_3 nanoparticles with high surface area were synthesized from $(NH_4)_3H_2W_{12}O_{40}$ or Na_2WO_4 via using mesoporous silica as a substrate[17] or a sol-gel process[18].

In this report, we have paid our attention to layered bismuth tungstate, $Bi_2W_2O_9$, as a precursor of WO_3 particles with high surface area. $Bi_2W_2O_9$ consists of alternately stacking anionic tungstate layers, $W_2O_7^{2-}$, and cationic bismuth oxide layer, $Bi_2O_2^{2+}$.[19, 20] Nano-sized $W_2O_7^{2-}$ layer having ReO_3 structure type tungsten trioxides interacts with nano-sized $Bi_2O_2^{2+}$ layer through the Coulomb's force, resulting in the alternate piled structures of $Bi_2W_2O_9$.

$Bi_2W_2O_9$ gives layered tungstate, $H_2W_2O_7$, by a treatment with hydrochloric acid.[21] (eqn. 1)

$$Bi_2W_2O_9 + 2HCl \rightarrow H_2W_2O_7 + Bi_2O_2^{2+} + 2Cl^- \quad (1)$$

, where bismuth oxide layers are eluted into a liquid phase. According to the TG data of $H_2W_2O_7$, the loss of interlayer hydration water occurs below 120 °C and $H_2W_2O_7$ is converted

---

[a] Department of Applied Chemistry, Tokyo Institute of Technology, 2-12 Ookayama, Meguro, Tokyo 152-8552, Japan. Fax: +81-3-5734-2879; Tel: +81-3-5734-2879; E-mail: yuji-w@apc.titech.ac.jp

[b] Research Fellow of Japan Society for the Promotion of Science.

[c] Present address: Interdisciplinary Cluster for Cutting Edge Research, Center for Energy and Environmental Science, Shinshu University, 3-15-1 Tokida, Ueda, Nagano 386-8567, Japan.

† Electronic Supplementary Information (ESI) available: Adsorption isotherms of WO_3 crystals, XRD patterns of $H_2W_2O_7$ and mosaic WO_3 reacted with n-octylamine, time change of temperature of reaction mixture at 80 °C, EDX spectrum of $Bi_2W_2O_9$, See DOI: 10.1039/b000000x/

into WO_3 via dehydration of the hydroxyl groups above 180 °C.[21] (eqn. 2)

$$H_2W_2O_7 \rightarrow 2WO_3 + H_2O \quad (2)$$

Moreover, we have conceived an idea that microwave irradiation can assist the preparation of the WO_3 particles with high surface area. Microwave irradiation as a heating method was popularly used for inorganic synthesis, exhibiting some advantages such as shortening the reaction time[22, 23] or controlling of morphology of the produced compounds[24-26]. These advantages of microwave methods are attributed to characters of microwave heating; rapid heating or substance-selective heating. The rapid heating is caused by heat generation in the irradiated substances through the loss of microwave energy. The selective heating is observed for an object consisting of two or more substances that have much different microwave loss factors (tan δ). When such object is irradiated with microwaves, a substance with greater tan δ value is heated more efficiently than that with lower tan δ, resulting in a large temperature gradient in the object. This phenomenon was directly observed by Raman spectroscopy in Tsukahara's work.[27] Recently, Maitani *et al*. found a specific microwave heating phenomenon observed at the interface of two different materials.[28] TiO_2 paste coated on a fluorine-doped tin oxide film is heated up efficiently under microwave irradiation, in which the heat is assumed to be generated locally at the interface between the two substances. This characteristic heating by microwave irradiation might be related to "interfacial dipolar relaxation" proposed elsewhere.[29]

We can find an example in which microwaves enhances synthesis of WO_3.[30] Spitzer *et al*. reported that the nanoparticles synthesized using the microwave heating have a larger specific surface area and smaller particle sizes than by the conventional heating in the hydrothermal method using WCl_6 as a precursor.[31] Particle size control of WO_3 by microwaves can be attributed to selective heating of seed crystals of WO_3, when it is taken into account that tungsten trioxides (WO_3) have great tan δ value (0.5 at 1.8 GHz, 0.436 at 9.14 GHz).[32, 33]

This paper reports a new synthesis of WO_3 particles using $Bi_2W_2O_9$ as a starting material under microwave irradiation. The effects of microwave heating on the morphology of the generated WO_3 particles are investigated in comparison with conventional heating. The replacement of $Bi_2O_2^{2+}$ with protons is accelerated by the effects of microwave heating, giving $H_2W_2O_7$, which is further converted to WO_3 at the last stage. A mechanism of the chemical transformation of $Bi_2W_2O_9$ under microwave irradiation is proposed based on the sequential observations of $Bi_2W_2O_9$ by SEM. WO_3 particles with large surface area synthesized under microwave irradiation show high photo-catalytic activity for decomposition of gaseous acetaldehyde. Specific effects of microwaves on the chemical transformation of $Bi_2W_2O_9$ are discussed especially focused on the substance-selective heating and interfacial dipole heating for the layered $Bi_2W_2O_9$ with extremely large interfacial area between $W_2O_7^{2-}$ and $Bi_2O_2^{2+}$.

Experimental

Chemical reagents

All the chemicals were reagent grade, and used as supplied. Bismuth (III) oxide (99.9%), hydrochloric acid, octylamine (98.0+%), heptane (99.0+%), methanol and $H_2PtCl_6 \cdot 6H_2O$ were purchased from Wako Pure Chemical Industries, Ltd. Tungsten (VI) oxide (99.99%) was purchased from High Purity Materials KOJUNDO CHEMICAL LABORATORY Co., Ltd. Water was purified by a Millipore Direct-Q 3 Ultrapure Water System to a resistivity of 18.2 MΩ cm.

Preparation of $Bi_2W_2O_9$

$Bi_2W_2O_9$ was obtained from the reported procedure.[19] Bismuth (III) oxide (3.02 g) and Tungsten (VI) oxide (3.00 g) were mixed by a pestle and mortar. The mixture powder was put in a platinum crucible and calcined at 800 °C for 48 h. Then, the resulting powder was identified as $Bi_2W_2O_9$ by XRD measurement as shown in Fig. 1(a). The EDX spectrum shown therein shows only the sharp peaks attributed to $Bi_2W_2O_9$, ensuring the high purity of $Bi_2W_2O_9$ (Fig. S2).

Hydrochloric acid treatment at 200 °C

$Bi_2W_2O_9$ (200 mg) suspended in 6 M hydrochloric acid (40 mL) was put into a Teflon (R) autoclave reactor with the volume of 80 mL. Then the reactor was heated at 200 °C. Microwave heating was carried out by Microsynth (Milestone Inc.). The rate of temperature rise was 40 °C/min under microwaves. After the temperature reached 200 °C, the samples were maintained at the temperature during various minutes, and then cooled to room temperature. Conventional heating was carried out using a hydrothermal synthesis reactor unit (HIRO COMPANY). The sealed Teflon (R) autoclave was put into the reactor unit heated at 200 °C. After various hours, the autoclave was cooled to room temperature. The reaction product was filtered and dried at 40 °C under vacuum several hours, and then the acid treated samples were obtained.

Hydrochloric acid treatment at 80 °C

$Bi_2W_2O_9$ (20 mg) suspended in water (2.0 mL) was pre-heated at 80 °C. Then, 12 M hydrochloric acid (2.0 mL) was injected into the above suspension solution. The sample solutions were collected 1, 2, 3, 5 min after HCl was injected. The sampled solutions were centrifuged and dried at 40 °C under vacuum several hours, and then the acid treated samples were obtained. The reaction vessels were Pyrex (R) test tubes with 18 mm inner diameter. A microwave irradiation system with an ellipsoidal chamber (CHRONICS) was used for microwave heating and, on the other hand, an oil bath was used for conventional heating. The reaction solutions were stirred by a mechanical stirrer with a stirring bar shaped like a flat-blade screwdriver. The stirring speed was set as 200 rpm. Reaction temperatures were measured by a fiber-optic thermometer (Opsens, Picosens).

n-Octylamine intercalation

n-Octylamine was intercalated into layered tungstate as previously reported.[21] The powder obtained by the hydrochloric acid treatment (100 mg) was suspended in a mixture of heptane (2.0 mL) and n-octylamine (1.0 mL), and stirred at room temperature. After 4 h, the suspension was centrifuged and washed by acetone several times and dried at 40 °C under vacuum several hours, and then the intercalated samples were obtained.

Photo-catalytic reaction

Visible light irradiation was performed by a 300 W Xe lamp (MAX-302; Asahi Spectra Co., Ltd.) equipped with a 400 nm cut-off filter. Pt co-catalyst was deposited on synthesized WO_3 particles by the reported photo-deposition method.[11] The acid treated WO_3 particles (100 mg) were dispersed into water, and $H_2PtCl_2 \cdot H_2O$ (2.65 mg corresponding to the amount of 1wt % of Pt on WO_3) was added into the dispersion. The dispersion was stirred and irradiated with λ>400 nm light. After 2 hour irradiation, methanol was added and then the dispersion was irradiated with λ>400 nm light for additional 2 hours. The dispersion was centrifuged, washed by acetone several times and dried at 40 °C under vacuum several hours, and then Pt supported WO_3 particles were obtained.

Photo-catalytic decomposition of gaseous acetic acid was performed in a Pyrex reaction vessel with the internal volume of 320 mL. The Pt supported WO_3 particles were spread on the flat bottom of the reaction vessel. Liquid acetic acid (15 μmol corresponding to the concentration of ca. 1000 ppm) was introduced into the vessel. The Pt supported WO_3 particles spread on the bottom was irradiated with λ>400 nm light through the bottom. The components in the gas phase were analysed by FID gas chromatography (Simadzu, GC-16A equipped with an Inart Cap Wax capillary column).

Characterization

X-ray diffraction spectra were collected by using desktop x-ray diffractometer Miniflex (RIGAKU) with bent monochromated CuKα radiation. Scanning electron microscopy (SEM) images were collected by a Hitachi S-5500 scanning electron microscope equipped with an energy dispersive x-ray spectroscope (EDX). Nitrogen adsorption measurements were performed on a Belsorp-mini (BEL JAPAN) sorption analyser. Prior to the sorption measurements, the samples were purged by N_2 gas at 423 K.

Results and discussion

$H_2W_2O_7$ is produced through eqn.1 when $Bi_2W_2O_9$ is treated with HCl at 80 °C under ambient pressure. This treatment induces elution of the $Bi_2O_2^{2+}$ layers and its substitution with H^+. We carried out the treatment experiments at 80 °C to slow down the rate of eqn.1 involved as the first step in the whole reaction from $Bi_2W_2O_9$ + 2HCl to WO_3 for discussing the whole reaction performed at 200 °C described later. Fig. 1 shows the XRD patterns and SEM images of the starting material of $Bi_2W_2O_9$ and the products after the HCl treatment at 80 °C for 1 h under both microwave heating and conventional heating. A peak at 2θ=7.5 ° (d=1.2 nm) observed in the XRD pattern of $Bi_2W_2O_9$ (Fig. 1a-(i)) was attributed to reflection of the layered structure of $Bi_2W_2O_9$.[19] This pattern was changed to those shown in Fig. 1a-(ii), (iii) after the treatment with HCl at 80 °C for 1 h under both microwave heating and conventional heating, respectively. A new peak observed at 2θ=9.1 ° (d=0.96 nm) was attributed to the layered structure of $H_2W_2O_7$ formed by the elution of the $Bi_2O_2^{2+}$ layers and its substitution with H^+.[21] The decrease of the d value after the treatment with HCl was caused by replacement of $Bi_2O_2^{2+}$ to H^+.

In order to confirm the layered structures of the resulting $H_2W_2O_7$, it was kept in contact with n-octylamine (Fig. S1(a), (b)). The treatment of $H_2W_2O_7$ with n-octylamine induced the shift of the peak at 2θ=9.1° to 3.3°, corresponding to the expansion of the interlayer gap through the intercalation with n-octylamine by 1.7 nm. Fig. 1b shows the SEM images of the same samples as examined by XRD. No difference in the appearances of the particles was observed after the treatment with HCl at 80 °C for 1 h under both microwave heating and conventional heating.

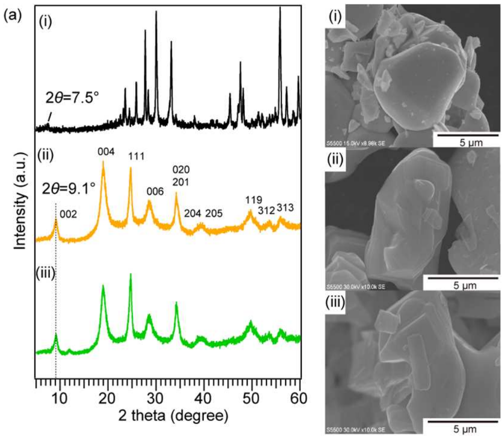

Fig. 1 (a) XRD patterns of (i) $Bi_2W_2O_9$, (ii) $Bi_2W_2O_9$ treated with HCl for 1 h at 80 °C under microwave heating and (iii) $Bi_2W_2O_9$ treated with HCl for 1 h at 80 °C under conventional heating. (b) SEM image of (i) $Bi_2W_2O_9$, (ii) $Bi_2W_2O_9$ treated with HCl for 1 h at 80 °C under microwave heating and (iii) $Bi_2W_2O_9$ treated with HCl for 1 h at 80 °C under conventional heating.

WO_3 is produced successively through eqn. 1 and eqn. 2 when $Bi_2W_2O_9$ is treated with HCl at 200 °C. This treatment induces elution of $Bi_2O_2^{2+}$ layers (eqn. 1) and successive dehydration reaction of $H_2W_2O_7$ (eqn. 2).[21] Fig. 2 shows the change of the XRD patterns of the products after the HCl treatment at 200 °C under microwave heating for 1 hour and conventional heating for 4 hour. All the peaks in these XRD patterns were attributed to monoclinic WO_3 (JCPDS 43-1035). These XRD patterns were not changed after treatment with n-octylamine (Fig. S1c), indicating that the products possessed no layered structure. A peak at 2θ=18° in Fig. 2a-(i) can be also attributed to the (004) plain of $H_2W_2O_7$ since the peaks observed at 2θ=18° in Fig. 1a-(ii) and (iii) are attributed to the (004) plain of $H_2W_2O_7$. The (004) peak of $H_2W_2O_7$ is derived from the layered structure. Because the intermediate of the reaction of $Bi_2W_2O_9$ with HCl at 200 °C is $H_2W_2O_7$ (see eqn. 1), the sample obtained by hydrothermal reaction of $Bi_2W_2O_9$ with HCl at 200 °C under microwaves can contain $H_2W_2O_7$ as an intermediate.

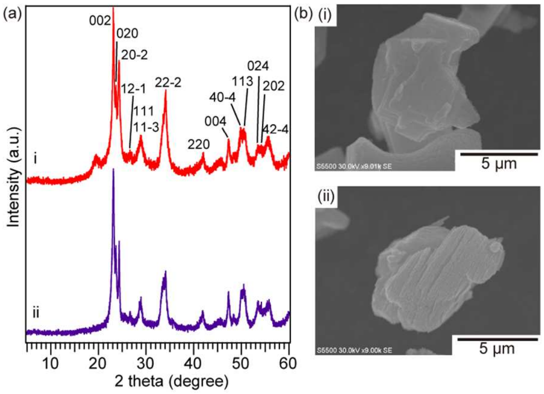

Fig. 2 (a) XRD patterns of (i) $Bi_2W_2O_9$ treated with HCl for 1 h at 200 °C under microwave heating and (ii) $Bi_2W_2O_9$ treated with HCl for 4 h at 200 °C under conventional heating. (b) SEM images of (i) $Bi_2W_2O_9$ treated with HCl for 1 h at 200 °C under microwave heating and (ii) $Bi_2W_2O_9$ treated with HCl for 4 h at 200 °C under conventional heating.

Then, we observed the morphological variations of WO_3 produced by $Bi_2W_2O_9$ treated with HCl at 200 °C by SEM. The SEM image shown in Fig. 3a shows two cracks on the surface of the products obtained by the treatment for 5min under microwaves. The enlarged SEM image (Fig. 3b) demonstrates more clearly the cracks and striped patterns derived from the layered structure of the precursor remaining at the lateral face of the particles with the plate-like shape. These cracks were thought to be generated by volumetric shrinkage during the dehydration reaction of $H_2W_2O_7$. After 30 min treatment under microwaves (Fig. 3c, d), the product had perforated structure with many rectangular holes. The particles looked like a sediment of the nano-size platelets with the width of ca. 100 nm (Fig. 3d). After 60 min treatment under microwaves, mosaic patterns with many rectangular holes at the whole area of the particles were observed (Fig. 3e) on the planes of the particles. We denote this product as mosaic-patterned WO_3 considering the identification of the compound by XRD shown in Fig 2. By comparing with the products obtained by 30 min treatment (Fig. 3 c), the mosaic-patterned WO_3 particles obtained by 60 min treatment had the fine and neat patterns of rectangular holes on the surface. The particles looked like a sediment of the nano-size platelet with the width of ca. 50 nm (Fig. 3f). The morphology of the product was extremely changed by 120 min treatment. Fig. 3g shows that flake-ball like WO_3 particles with a diameter of 500 nm were aggregated on the large WO_3 particles. The flake-ball like particles should be formed by re-aggregation of dispersed flake chips produced through the formation of the rectangular holes.

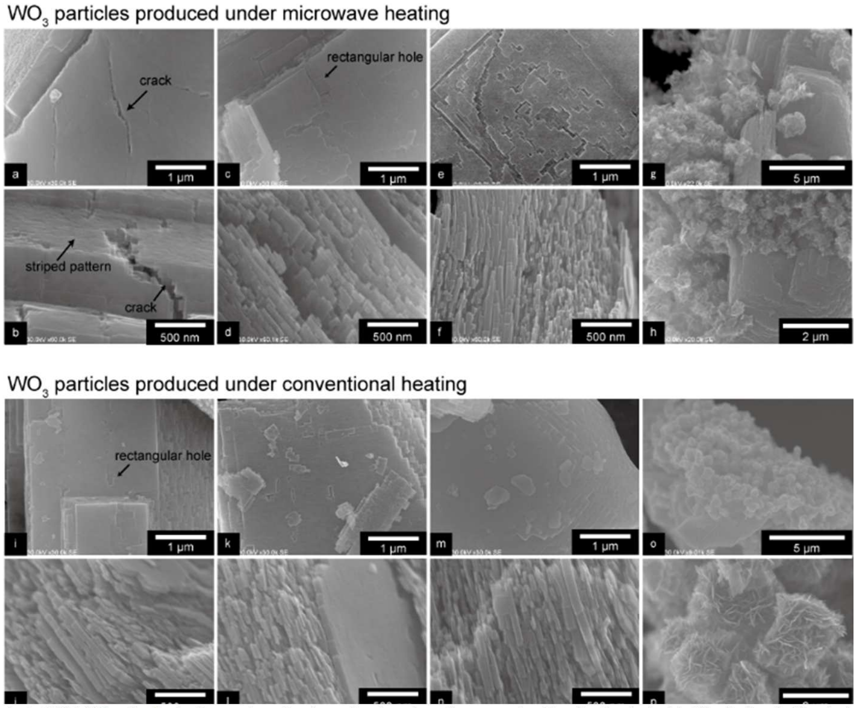

Fig. 3 SEM images of WO_3 treated at 200 °C by the hydrothermal synthesis method under microwave heating for 5 min (a, b), 30 min (c, d), 60 min (e, f), 120 min (g, h), and under conventional heating for 2 h (i, j), 4 h (k, l), 6 h (m, n), 12 h (o, p)

The SEM images in Fig. 3i-p show the morphology variations of WO_3 produced under conventional heating at 200 °C. The products obtained by 2, 4 or 6 hour treatment under conventional heating had the rectangular holes at the surface of WO_3 particles (Fig. 3i, k, m). However, comparing with WO_3 particles obtained by microwave heating, extremely few holes were found on the surface. The particles observed in these images had flat surface and plate-like structures. After 12 hour treatment under conventional heating, the flake-ball like particles were partially formed (Fig. 3o, p).

The sequential SEM observations indicated that the morphology of the produced WO_3 particles was changed according to the reaction time and heating method. Taking into account these observations, we propose a scheme of the morphological variation of $Bi_2W_2O_9$ treated with HCl under microwave heating and conventional heating (Fig. 4). By microwave heating, the starting material, $Bi_2W_2O_9$, was changed to WO_3 particles with plate-like structure at the very early stage of the reaction. And then, the morphology of the WO_3 was transformed into the mosaic structure over 60 min of the treatment. After 120 min of the treatment under microwaves, the WO_3 particles with flake-ball structure were produced. On the other hand, under conventional heating, WO_3 particles with plate-like structure were also produced at first, and then these were converted to WO_3 particles with flake-ball structure over 12 h of the reaction. Under conventional heating, WO_3 particles with mosaic patterns were not absolutely observed. This is the first microwave effect observed in the reaction of $Bi_2W_2O_9$ to WO_3 particles in acidic conditions. Furthermore, the accelerated transformation of WO_3 particles with plate-like structure to WO_3 particles with flake-ball structure should be emphasized as another second microwave effect.

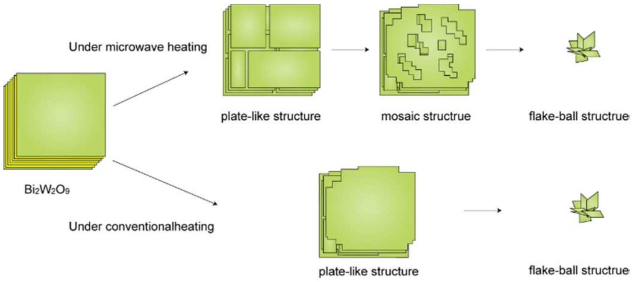

Fig. 4 Scheme for morphological variation of WO_3 produced by $Bi_2W_2O_9$ treated with hydrochloric acid under microwave heating and conventional heating.

We examined the effect of microwave irradiation on the elution of $Bi_2O_2^{2+}$ (eqn. 1). The elution rate of $Bi_2O_2^{2+}$ under microwave heating was compared with the rate under conventional heating. The Bi/W ratios in the samples were determined using the peak areas of Bi Lα line at 10.84 eV and W Lα line at 8.40 eV in the EDX spectrum, considering the detection sensitivities of both elements. The Bi/W ratio of 1.0 was obtained for $Bi_2W_2O_9$ as the starting compound using the EDX spectrum shown in Fig. S2 and decreased with the progress of the treatment time. Here, the Bi/W ratio values were the mean value for the five particles observed in the SEM image. It should be noticed here that the EDX spectrum reflects the elemental information of the surface layer with the depth of 1 μm of the measurement samples.

The Bi/W ratios determined by the above EDX method for the samples treated with HCl were decreased with the progress of the reaction time under microwave heating and conventional heating as shown as in Fig. 5, indicating the elution of $Bi_2O_2^{2+}$ during the treatment. The initial rate of the decrease in the Bi/W ratio under microwave heating was about 2 times faster than that under conventional heating. The acceleration of the elution reaction of $Bi_2O_2^{2+}$ by microwave heating can be an origin of the microwave effects observed in the morphology variations observed above in the SEM images.

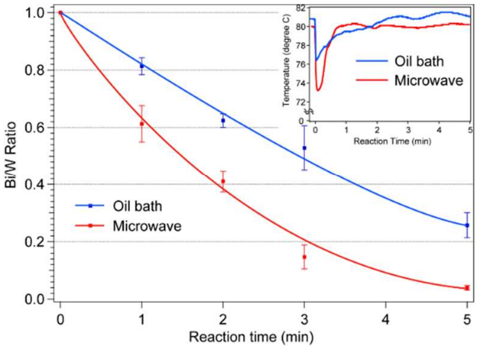

Fig. 5 Time variation of the Bi/W ratios over hydrochloric acid treatment of $Bi_2W_2O_9$ under microwave heating (red plots) and oil-bath heating (blue plots). Inset: Temperature changes of the reaction solution containing 6 M hydrochloric acid (4.0 mL) and $Bi_2W_2O_9$ (20 mg) under microwave heating and oil bath heating.

The temperature of the reaction mixture was measured by using a fiber-optic thermometer (Opsens, Picosens) during microwave and conventional heating. Changes of the temperatures are shown in Fig. 5 inset with the heating time. Before starting the reaction by injecting HCl aq, the temperatures of the reaction mixtures were maintained at 80.0~80.8 °C. When the HCl was injected into the reaction mixtures at 0 min (the reaction was started at this time), the temperatures of the reaction mixtures were dropped to 73~76 °C. However, the temperatures of both reaction mixtures under microwave irradiation and conventional heating were recovered to 80°C within 2 minutes and precisely controlled at 80 ± 1.5°C. We would add that the temperature of the reaction mixture under microwaves was even lower than conventional heating, except for 0.5 ~ 1.5 min. Then, the accelerated elution of the $Bi_2O_2^{2+}$ under microwave irradiation can be hardly explained as due to the temperature difference of the reaction mixtures. We propose here that the acceleration should be attributed to the selective heating at $W_2O_7^{2-}$ layers or the interface between $W_2O_7^{2-}$ layers and $Bi_2O_2^{2+}$ layers. Our group reported the special heating of the interface between a TiO_2 paste and a fluorine doped SnO_2 film.[28] The similar interfacial heating can be induced for the present case under microwave irradiation. The temperature distribution caused by such interfacial heating under microwaves can induce higher temperature of the $Bi_2O_2^{2+}$ layers than the surroundings, resulting in the accelerated elution of $Bi_2O_2^{2+}$ layers (eqn. 1).

Furthermore, $Bi_2W_2O_9$ particle might experience the selective heating effect by the interaction with microwave alternative electromagnetic field. The temperature of the inner part of the particles can be higher than the outer surface through the interactions.[34, 35]

On the other hand, under conventional heating, the $Bi_2W_2O_9$ particles were heated by heat transfer from the surroundings, and then the temperature distribution of the particles and the surroundings should be homogeneous supposing that the heat equilibrium is reached. The difference in the temperature distribution between microwave irradiation and conventional heating should lead to the difference in the dynamics of the elution of $Bi_2O_2^{2+}$ (eqn. (1)) and the dehydration reaction of $H_2W_2O_7$ (eqn. (2)) at the inner particle and outer surface. It might explain why WO_3 particles with mosaic patterns was produced only under microwaves.

The BET specific surface areas and morphologies of the WO_3 particles obtained by treatment of $Bi_2W_2O_9$ with HCl at 200 ° C are summarized in Table 1. The adsorption isotherms of the WO_3 particles produced by microwave and conventional heating are shown in Fig. S3 and Fig. S4, respectively. Under microwave heating, as the reaction time increased from 5 min to 60 min, the surface area of the WO_3 particles increased from 12.3 to 51.8 m^2 g^{-1}. This increase in the surface area agreed to the changes in the morphology of the particles observed in the SEM images. However, the surface area of the WO_3 particles obtained by 120 min acid treatment was smaller than that of 60 min treatment. In the SEM observation, the structure of the WO_3 particles obtained by 60 min treatment was mosaic, while that obtained by 120 min treatment was flake ball. Therefore, it is mentioned that the structure with the mosaic patterns has large surface area compared to flake ball structure, probably due to the much porosity of the structure with the mosaic patterns.

Table 1. BET surface area, morphology and photocatalytic activity data of WO_3 produced by $Bi_2W_2O_9$ treated with HCl under at 200 °C by the hydrothermal synthesis method.

Synthesis method	Treatment time	BET surf. area/m^2 g^{-1}	Morphology	Photocatalytic acetaldehyde decomposition rate/μmol h^{-1} g^{-1}
Microwave hydrothermal	5 min	12.3	plate-like	427
	30 min	20.8	plate-like	
	60 min	51.8	mosaic	
	120 min	18.6	flake-ball	
Conventional hydrothermal	2 h	11.1	plate-like	408
	4 h	32.2	plate-like	
	6 h	11.3	plate-like	
	12 h	22.2	flake-ball	
Purchased WO_3		7.54		147

The diffuse reflectance spectra of flake-ball WO_3 produced by $Bi_2W_2O_9$ treated with HCl for 12 h at 200 °C under conventional heating and mosaic-patterned WO_3 produced by $Bi_2W_2O_9$ treated with HCl for 60 min at 200 °C under microwave heating are shown in Fig. 6. The band gap energy of the flake-ball (2.71 eV) WO_3 was larger than that of mosaic-patterned WO_3 (2.62 eV). The band gap energy of bulk WO_3 is 2.6 eV.[17] Increase in the band gap energy of flake-ball WO_3 should be attributed to the quantum size effect. Then, the average crystallite diameter $D(hkl)$ was estimated from XRD pattern by using Scherrer's equation.

$$D(hkl) = \frac{0.94\lambda}{\beta \cos\theta}$$

, where is λ is the X-ray wavelength, β is the full width at half maximum of X-ray diffraction peak in radian and θ is the Bragg's angle of the diffraction peak. Here, the (002) peak with the highest intensity was selected to evaluate the crystallite diameter. The crystallite diameters of mosaic-patterned WO_3 and flake-ball WO_3 were calculated to be 31.3 nm and 21.6 nm, respectively, suggesting occurrence of the quantum size effect for flake-ball WO_3.

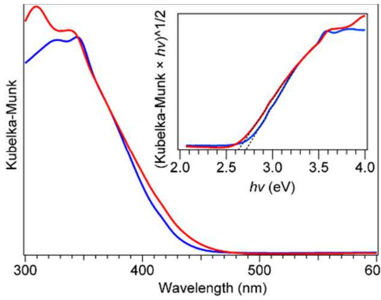

Fig 6 Diffuse reflectance spectra of mosaic-patterned WO_3 particles produced by $Bi_2W_2O_9$ treated with HCl for 60 min at 200 °C under microwave heating (red), and WO_3 flake-ball particles produced by $Bi_2W_2O_9$ treated with HCl for 12 h at 200 °C under conventional heating (blue).

To evaluate the photocatalytic activity of the WO_3 particles prepared in this work, the decomposition reaction of gaseous acetaldehyde was investigated for the samples obtained by microwave heating for 60 min (mosaic-patterned WO_3 with the BET surface area 51.8 m^2 g^{-1}), obtained by the conventional heating for 4 h (BET surface area 32.2 m^2 g^{-1}) and commercially available WO_3 particles (BET surface area 7.54 m^2 g^{-1}) (Fig. 7). 1 wt% Pt particles of about 5 nm particle size were supported on these WO_3 particles by a pre-known method.[11] Both WO_3 particles obtained by microwave and conventional heating showed higher photocatalytic activity than the commercial WO_3 particles. The high catalytic activities were attributed to the high specific surface area of the particles prepared in this work. No large difference in the photocatalytic activity was observed between both particles obtained microwave irradiation and conventional heating.

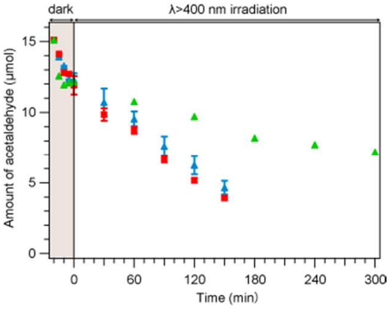

Fig. 7 Photocatalytic decomposition of gaseous acetaldehyde over purchased WO_3 (green plots), mosaic-patterned WO_3 particles by $Bi_2W_2O_9$ treated with HCl for 1 h at 200 °C under microwave heating (red plots) and plate-like WO_3 particles produced by $Bi_2W_2O_9$ treated with HCl for 4h at 200 °C under conventional heating (blue plots).

Conclusions

WO_3 particles of mosaic patterns with high specific surface area (51.8 m^2 g^{-1}) were obtained by hydrochloric acid treatment of $Bi_2W_2O_9$ at 200 °C under microwave heating. Mosaic-patterned WO_3 particles obtained by only microwave heating were converted into WO_3 particles with flake-ball shape by the prolonged irradiation. Flake-ball WO_3 was obtained both for microwave heating and conventional heating, but the whole process of the transformation from $Bi_2W_2O_9$ to WO_3 was much shortened by using microwave irradiation. We have demonstrated that the elution of $Bi_2O_2^{2+}$ layer was accelerated by microwave heating. This accelerated elusion observed under microwave irradiation can be attributed to the selective heating at $W_2O_7^{2-}$ layers or the interface between $W_2O_7^{2-}$ layer and $Bi_2O_2^{2+}$ layer through the interaction of $Bi_2W_2O_9$ with microwave alternative electromagnetic field. Photocatalytic decomposition of gaseous acetaldehyde under visible light irradiation was examined for the WO_3 particles prepared in this work. Mosaic-patterned WO_3 particles obtained by microwave heating showed 2.9 times higher photocatalytic activity than a commercially available WO_3 particles (BET surface area 7.54 m^2 g^{-1}) and 1.05 times higher the photocatalytic activity than WO_3 particles obtained by conventional heating (BET surface area 32.2 m^2 g^{-1}).

Acknowledgements

We thank S. Genseki and K. Hori (Tokyo Institute of Technology) for TEM observations. This study was supported in part by Grant-in-Aid for Scientific Research (A) 25249113, Grant-in-Aid for Exploratory Research, and Grant-in-Aid for Young Scientists (B) from MEXT, Japan, ASPIRE League Research Grant 2014 and 2015, Tokyo Tech, Research Grant of TEPCO Memorial Foundation, and Demonstration and Standardization Project Using New Electric Devices, NEDO.

Notes and references

1 G. Hodes, D. Cahen and J. Manassen, *Nature*, 1976, **260**, 312.
2 K. L. Hardee and A. J. Bard, *J. Electrochem. Soc.*, 1977, **124**, 215.
3 J. R. Darwent and A. Mills, *J. Chem. Soc., Faraday Trans.*, 1982, **78**, 359.
4 H. Wang, T. Deutsch and J. Tumer, *J. Electrochem. Soc.*, 2008, **155**, F91.
5 M. R. Waller, T. K. Townsend, J. Zhao, E. M. Sabio, R. L. Chamousis, N. D. Browning and F. E. Osterloh. *Chem. Mater.*, 2012, **24**, 698.
6 K. Sayama, R. Yoshida, H. Kusama, K. Okabe, Y. Abe and H. Arakawa, *Chem. Phys. Lett.*, 1997, **277**, 387
7 A.Kudo, H. Kato and I. Tsuji, *Chem. Lett.*, 2004, **33**, 1534.
8 X. Chen, S. Shen, L. Guo and S. S. Mao, *Chem. Rev.*, 2010, **110**, 6503.
9 K. Maeda, M. Higashi, D. Lu, R. Abe and K. Domen, *J. Am. Chem. Soc.*, 2010, **132**, 5858.
10 H. N. Kim, T. W. Kim, K. H. Choi, I. Y. Kim, Y. R. Kim and S. J. Hwang, *Chem. Eur. J.*, 2011, **17**, 9626.
11 R. Abe, H. Takami, N. Murakami and B. Ohtani, *J. Am. Chem. Soc.*, 2008, **130**, 7780.
12 F. Amano, K. Nogami, R. Abe and B. Ohtani, *J. Phys. Chem. C*, 2008, **112**, 9320.
13 F. Amano, K. Nogami and B. Ohtani, *J. Phys. Chem. C*, 2009, **113**, 1536.
14 M. Sadakane, N. Tamura, N. Kanome, S. Sumiya, R. Abe and T. Sano, *Chem. Lett.*, 2011, **40**, 443.
15 M. Sadakane, K. Sasaki, H. Kunioku, B. Ohtani, R. Abe and W. Ueda, *J. Mater. Chem.*, 2010, **20**, 1811.
16 M. Sadakane, K. Sasaki, H. Nakamura, T. Yamamoto, W. Ninomiya and W. Ueda, *Langmuir*, 2012, **28**, 17766.
17 D. Tanaka, Y. Aoki and H. Imai, *Chem. Comm.*, 2010, **46**, 5286.
18 Z. Lu, S. M. Kanan and C. P. Tripp, *J. Mater. Chem.*, 2002, **12**, 983.
19 Y. Bando, A. Watanabe, Y. Sekikawa, M. Goto and S. Horiuchi, *Acta Cryst.*, 1979, **A35**, 142.
20 J.-C. Champarnaud-Mesjard, B. Frit and A. Watanabe, *J. Mater. Chem.*, 1999, **9**, 1319.
21 M. Kudo, H. Ohkawa, W. Sugimoto, N. Kumada, Z. Liu, O. Terasaki and Y. Sugahara, *Inorg. Chem.*, 2003, **42**, 4479.
22 R. Gedye, F. Smith, K. Westway, H. Ali, L. Laberge, R.Rousell, *Tetrahedron Lett.*, 1986, **27**, 279.
23 C. O. Kappe, *Angew. Chem. Int. Ed.*, 2004, **43**, 6250.
24 N. N. Mallikarjuna and R. S. Varma, *Crystal Growth & Design*, 2007, **7**, 687.
25 D. Dambournet, A. Demourgues, C. Martineau, S. Pechev, J. Lhoste, J. Majimel, A. Vimont, J. C. Lavalley, C. Legein, J. Y. Buzare, F. Fayon and A. Tressaud, *Chem. Mater.*, 2008, **20**, 1459.
26 Z. Chen, D. Mochzuki, M. M. Maitani and Y. Wada, *Nanotechnology*, 2013, **24**, 265602.
27 Y. Tsukahara, A. Higashi, T. Yamauchi, T. Nakamura, M. Yasuda, A. Baba and Y. Wada, *J. Phys. Chem. C*, 2010, **114**, 8965.
28 M. M. Maitani, T. Inoue, Y. Tsukushi, N. D. Hansen, D. Mochizuki, E. Suzuki and Y. Wada, *Chem. Commun.,* 2013, **49**, 10841.
29 P. A. Miles, W. B. Westphal and A. von Hippel, *Rev. Mod. Phys.,* 1957, **29**, 279.
30 D. R. Baghurst and D. M. P. Mingos, *J. Chem. Soc., Chem. Commun.*, 1988, 829.
31 N. L. Houx, G. Pourroy, F. Camerel, M. Comet and D. Spitzer, *J. Phys. Chem. C,* 2010, **114**, 155.
32 J. Pfeifer, I. Csaba and K. Elek, *J. Solid State Chem.* 1994, **111**, 349.
33 R. Schmitt, D. McCann, B. Marquis and D. E. Kotecki, *J. Appl. Phys.*, 2002, **91**, 6775.
34 S. Fujii, H. Kujirai, D. Mochizuki, M. M. Maitani, E. Suzuki and Wada, *J Microwave Power Electromagnetic Energy*, 2014, **48**, 89.
35 D. Mochizuki, R. Sasaki, M. M. Maitani, M. Okamoto, E. Suzuki and Y. Wada, *J. Catal.*, 2015, **323**, 1.

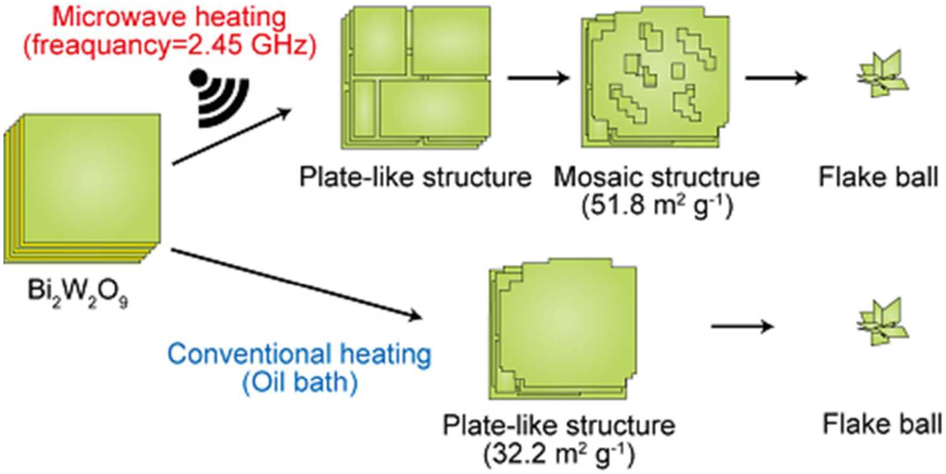

High surface area WO3 particles with mosaic patterned-structures were obtained under microwave irradiation.